OPEN ACCESS

GAVIN PUBLISHERS

Nanomedicine and Nanoscience Research

Research Article

Lapina V, et al. J Nanomed Nanosci: JNAN-157.

DOI: 10.29011/2577-1477. 100057

New Generation of Photosensitizers: The Conjugate of Folic Acid with Nanoparticles and Chlorine E6

V. Lapina*, T. Pavich, S. Bushuk, J. Kalvinkovskaya, A. Vorobey, B. Bushuk

B.I. Stepanov Institute of Physics of NAS Belarus, Minsk, Belarus

***Corresponding author:** V. Lapina, B.I. Stepanov Institute of Physics of NAS Belarus,68 Nezavisimosti Ave., 220072, Minsk, Belarus.Tel: +375-172842869; Fax: +375-172840879; Email: vlapina@dragon.bas-net.by

Citation: Lapina V, Pavich T, Bushuk S, Kalvinkovskaya J, Vorobey A, et al. (2018) New Generation of Photosensitizers: The Conjugate of Folic Acid with Nanoparticles and Chlorine E6. J Nanomed Nanosci: JNAN-157. DOI: 10.29011/2577-1477. 100057

Received Date: 22 December, 2018; **Accepted Date:** 24 January, 2019; **Published Date:** 30 January, 2019

Abstract

A new generation of selective photosensitizers based on nanodiamond particles has been developed. The possible ways of synthesis of conjugate comprising folic acid as a targeting vector, nanodiamond particles as carriers, chlorine e6 as a photosensitizer, have been demonstrated. Spectral-luminescent properties of the conjugates have been studied. It has been shown that the conjugate obtained effectively binds to cells in vitro. It was observed that chlorine e6 immobilized on ND particles reveals its photodynamic activity under illumination and induces death of cells. Based on obtained results, possible advanced therapeutic strategies for novel medical technologies have been proposed.

Keywords: Chlorine e6; Folic acid; Nanodiamond particle; Photodynamic therapy; Photosensitizers

List of Abbreviations

PDT	:	Photodynamic Therapy
FA	:	Folic Acid
ND	:	Nanodiamond
Che6	:	Chlorine E6
HeLa cells	:	Cervical Cancer Cells
DMSO	:	Dimethyl Sulfoxide
TBAEE	:	Tret-Butyl-N-{2-[2-(2-Aminoethoxy)Ethoxy]Ethylate}
DCC	:	Dicyclohexycarbodiimide
DMAP	:	4-Dimethylaminopyridine
CDI	:	1,1′-Carbonyldiimidazole
TFA	:	Trifluoroacetic Acid
DMFA	:	Dimethylformamide
THF	:	Tetrahydrofuran
DCM	:	Dichloromethane
PBS	:	Phosphate Buffered Saline
EDA	:	2, 2 -(Ethylenedioxy)Bis-(Ethylamine)

Introduction

One of the main factors determining the efficiency of Photodynamic Therapy (PDT) is the selectivity of photosensitizer accumulation in a tumor tissue as compared to healthy ones, which provides increased therapeutic effect along with reduced terms of treatment and decreased side toxic effect of corresponding drugs. That is why at present efforts are made aimed at the creation of the methods for selective photosensitizer delivery of into tumor cells. The use of cytotoxic agents conjugated to highly specific tumor cell plasmatic membrane receptor ligands is very promising for such selective delivery. Monoclonal antibodies, oncofetal proteins, transferrin, hormone-like peptides, etc. are often used as such ligands.

Folic Acid (FA) is a highly efficient ligand providing selective delivery and introduction of chemotherapeutic drugs into proliferative-active cells [1,2]. FA is a vitamin, which after enzymatic cellular recovery acts as a cofactor of key synthesis ferments of nucleic acids bases and some amino acids. That is why proliferatively active, quickly dividing cells express large amounts of FA receptors having rather high affinity to the substrate. The important circumstance is that the expression of folate receptor by the transformed cells increases in later stages of tumor process that allows using folate-mediated therapy of tumors in cases which are difficult to treat using ordinary methods of chemotherapy. At

the same time the cells of normal tissues express rather small or indeterminable quantity of folic receptors on their surface [3-5]. The exclusions are the cells of kidney, placenta, epithelial cells of a lung, vascular membranes and some other organs. Different types of malignant transformed cells, particularly, cells of tumors of lung, kidney, brain, large intestine, ovary, uterus, orchis, myelocytic blood cells in leukemia have on their surface a large number of folate receptors [6,7]. These folate receptor positive cells bind folates efficiently in essential quantities (more than 6×10^7 molecules per cell) [8].

Of profound interest is the possibility of using folate-mediated photosensitizer delivery into folate receptor positive tumor cells for photodynamic therapy of tumors. The first attempts of increasing PDT selectivity were made using the conjugation of photosensitizers to monoclonal antibodies. As it is shown in [9], such conjugation of phthalocyanines being perspective substances for PDT increases essentially the efficiency of photodamage of tumor cells *in vitro* and *in vivo* due to selective accumulation of conjugated photosensitizer. The first report on the possibility of using folate-mediated endocytosis of photosensitizers aimed at the selective tumor cell delivery and the increased efficiency of photosensitized cellular damage appeared in 2005 [10]. On the folate receptor positive cells of K-W line (nasopharyngeal epidermal carcinoma) the authors showed that the efficiency of photodynamic inactivation of cells is ~3 times higher when using FA-conjugated tetraphenylporphyrin than in the case of free porphyrin. Cells are capable of capturing receptor-bound conjugates without their destruction by means of receptor-mediated endocytosis with the formation of endosomes [11].

Since the mechanism of folate receptor mediated endocytosis allows transmembrane transfer of macromolecules and even their aggregates [12], in many scientific centers the investigations are intensively conducted on the development of "endocytose" technologies of chemotherapeutic drugs introduction into pathologically changed cells using folate receptor (conjugation with folic acid). In clinical practice the successful delivery into folate receptor positive cells is already achieved for protein toxins, immune stimulants, chemotherapeutic agents, liposomes with bound ligands, nanoparticels and various diagnostic probes [13]. The first studies were dedicated to the selective delivery of anti-tumor antibiotic doxorubicin into folate receptor positive cells [14]. Today the rapid development of nanotechnologies offers significant challenges for the elaboration of new generation drugs, particularly, photodynamically active ones. The use of nanoparticles offers various possibilities for designing new generation drugs thanks to reasonable combination of physical, chemical (such as adsorption, chemistry of surface, activity, safety and so on) and biological properties of components compiling a drug.

At present, in order to increase general PDT efficiency photosensitizers are conjugated to nanoparticles of various nature (liposomes, dendrimers, fullerenes, quantum dots and others) [15]. Among new generation nanomaterials used for drug design, Nanodiamonds (ND) of denotation synthesis occupy a special place. At present a number of researchers use this material in different reactions of chemical synthesis (such as adsorption, covalent, fragmentary, linker binding and so on) to obtain new structures. Earlier we have shown that the conjugation of well-known and widely applied in clinical practice chlorine e6 (Che6) photosensitizer with diamond nanoparticles leads to the formation of efficient photodynamically active conjugate [16]. At the same time it was established [17] that ND particles conjugated with folic acid are efficiently bound to HeLa cells and can penetrate the cells. Taking into account the above mentioned considerations, it is reasonable to develop a selective conjugate containing also a vector ligand, particularly, FA, to increase PDT efficiency using Che6-ND. The purpose of the present investigation is to determine the potential possibility of the development of new generation selective photosensitizers at the example of synthesized three-component Che6-ND-FA nanocomplex.

Materials and Methods

In present study Che6 produced by UE "Dialek" (Minsk, Republic of Belarus) was used as a photosensitizer. Commercial ND samples were obtained from "Sinta" (Minsk, Republic of Belarus); Dimethyl Sulfoxide (DMSO), Tret-Butyl-N-{2-[2-(2-Aminoethoxy)Ethoxy]Ethylate} (TBAEE), Dicyclohexycarbodiimide (DCC), 4-Dimethylaminopyridine (DMAP), 1,1′-Carbonyldiimidazole (CDI), Trifluoroacetic Acid (TFA), Dimethylformamide (DMFA), Tetrahydrofuran (THF) and Dichloromethane (DCM) were obtained from Sigma-Aldrich (USA). The conjugates synthesized were dissolved in Phosphate Buffered Saline (PBS) (pH 7.4) containing DMSO (5%) in order to study the spectral properties and photosensitizing activity of free Che6 and that conjugated with ND. Absorption, fluorescence and fluorescence excitation spectra of free Che6 and conjugate suspensions were recorded at Che6 concentration of 4×10^{-7} mol/l and nanoparticle concentration of 0.014 mass %.

The photosensitizing activity of free Che6 and its conjugates was determined from their ability to sensitize photodestruction of Human Serum Albumin (HSA) tryptophan, which was determined from the intensity decrease of tryptophan fluorescence after illumination of the samples. The illumination was performed in a 1 cm cuvette by light from the KGM lamp (150W) through a water filter and FS4 bandpass filter transmitting light in the 370-430 nm spectral region. Absorption spectra were measured using Varian Cary 50 spectrophotometer (USA), fluorescence spectra - using Varian Cary Eclipse spectrofluorometer (USA).

Laser scanning confocal imaging was performed using Zeiss LSM 510 NLO microscope equipped with CW multiline Argon ion laser. Brightfield and fluorescence microscopic images were taken

using the same microscope in transmitted light and fluorescent microscopy regimes, respectively. In the latter case, the samples were excited by mercury lamp lines and fluorescence emission was collected using corresponding filtersets. Microspectroscopy was performed by LSM using ROI excitation and dedicated registration channel fiber-coupled to Acton SP-2500i spectrometer equipped with notch filter chamber and sensitive back-illuminated CCD camera Princeton Instruments Spec-10.

Synthesis of Chlorine E6 Conjugates with Diamond Nanoparticles and Folic Acid

In our work FA was used as a vector ligand with the purpose of receptor-mediated internalization of diagnostic and therapeutic agents into cells. Che6 was used as an efficient photosensitizing agent, ND of detonation synthesis as a nanoplatform carrying the molecules of photosensitizer as well as vector ligand from one side and from the other side as a linker between molecules of a photosensitizer and a vector agent. The synthesis of FA-ND-Che6 conjugate was performed on the basis of analysis of physical and chemical properties of nanodiamonds of detonation synthesis as well as Che6. (Figure 1) shows the structures of the components used for conjugate synthesis.

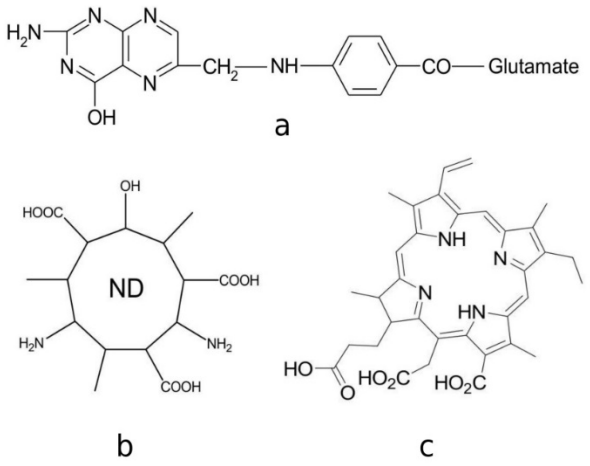

Figure 1: The structures of folic acid **(a),** nanodiamond **(b)** and chlorine e6 **(c).**

It is seen from the presented structures that every one of the structural units has functional groups suitable for conjugation. So the presence of reactive carboxyl groups in FA gives the possibility for the synthesis of their conjugates with different drugs. Usually to preserve the specificity and high affinity to cellular membrane receptors the conjugation was made using a linker allowing spatial separation of FA and cytotoxic drug. The use of ND gives the possibility to achieve the conjugation with and without a linker. In the second case ND can be treated not only as a carrier platform for photosensitizer molecules, but also as a linker between them. It is known that the determining factor for immobilization of various molecules (in our case molecules of Che6 and FA) on the surface of nanoparticles is their surface state, which is determined by such properties as purity, size of primary crystallites, their aggregates, chemistry and surface charge. For the conjugation of FA and Che6 with ND we have used the nanodiamonds which properties were analyzed according to commonly used techniques described in works [18,19] and are presented in (Table 1).

Characteristics	Measurement unit	ND samples (produced by "Sinta")
Average size of microcrystallites	nm	4-8
Average size of primary aggregates	nm	20-30
Specific surface	m^2/g	300-350
Electrokinetic potential (pH 7.36)	mV	-25
Total content of impurities	%	up to 0.3

Table 1: Properties of the nanodiamond powders used.

Taking into account the presence of carboxyl and amino groups in the shell of nanodiamond particles [20] as well as carboxyl groups in the structure of chlorine [21], it was reasonable to perform conjugation of these components using the mentioned groups. The conjugation of initial components using 2,2-(ethylenedioxy)bis-(ethylamine) (EDA) spacer was conducted in two stages [22]: 1. Joining the spacer to ND carboxyl groups. 2. Activation of carboxyl groups of FA and Che6 and their joining to spacer amino groups.

Obtaining ND-$(EDA)_n$ complex (Figure 1)

The ND suspension was prepared using the method described in the literature [23], and the ND-$(EDA)_n$ complex was prepared using the modified method described in paper [24]. The synthesis was conducted as follows: into 50-ml round-bottomed flask nanodiamond powder (50 mg) and 20 mg of anhydrous DMSO were added, then the suspension was stirred on a magnetic stirrer for 1 hour and dispersed for 10 min. The resulting colloid was treated with ultrasound for 40 minutes at 22 kHz. After processing of ND with ultrasound, DCC (248 mg; 1.2 mmol) and NHS (230 mg, 2.0 mmol) were added to the suspension and then the stirrer was kept for 6 hours at 50°C under intense stirring by magnetic stirrer. Then to the formed ND-NHS complex EDA (1480 mg, 10 mol) and pyridine (100 µl) were added and the mixture was stirred for 5 hours at 25°C. Further, the reaction mixture with the obtained ND-$(EDA)_n$ sediment was centrifuged (30 min at 10000 rev/min), then it was washed twice with 10 ml of ethyl ether and centrifuged. The obtained complex was used for further syntheses.

Synthesis of $(FA\text{-}spacer)_n$ -ND conjugate (Figure 2)

To the obtained complex 1 (10 mg) 10 mg of anhydrous DMSO were added, then it was allowed to disperse during 10 minutes in nitrogen atmosphere. After that FA was added activated as follows: to FA (4.4 mg; 0.01 mmol) in the mixture of anhydrous DMSO (5 ml) and pyridine (0.7 ml), CDI (2.0 mg; 0.012 mmol) was added and stirred for 1 hour at 25˚C on a magnetic stirrer in inert atmosphere. Further, the reaction mixture was stirred on a magnetic stirrer for 5 hours at room temperature. After termination of the reaction the resulting suspension was centrifuged (30 min at 10000 rev/min), and then repeatedly washed with 5 ml of DMSO and 10 ml of ethyl ether in turns and centrifuged. The $(FA\text{-}spacer)_n$-ND conjugate was used for spectral measurements.

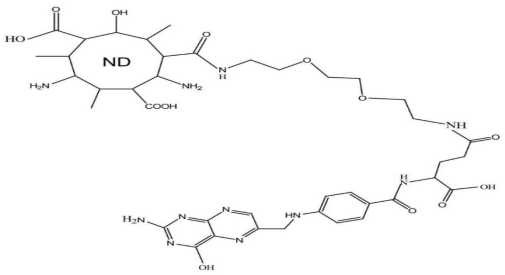

Figure 2: The structure of $(FA\text{-}spacer)_n$-ND conjugate.

Synthesis of the $(Che6\text{-}spacer)_n$-ND conjugate (Figure 3)

To the obtained complex 1 (10 mg) 10 mg of anhydrous DMSO were added, then it was dispersed for 10 minutes in nitrogen atmosphere. After that, Che6 was added activated as follows: to Che6 (5.9 mg; 0.01 mmol) in the mixture of anhydrous DMSO (5 ml) and pyridine (0.7 ml) CDI (2.0 mg; 0.012 mmol) was added and stirred for 1 hour at 25˚C on a magnetic stirrer in an inert atmosphere. Further, the reaction mixture was stirred on a magnetic stirrer for 5 hours at room temperature. After termination of the reaction the resulting suspension was centrifuged (30 min at 10000 rev/min), repeatedly washed with 5 ml of DMSO and 10 ml of ethyl ether in turns and centrifuged. The Che6-spacer-ND conjugate was also used for spectral measurements.

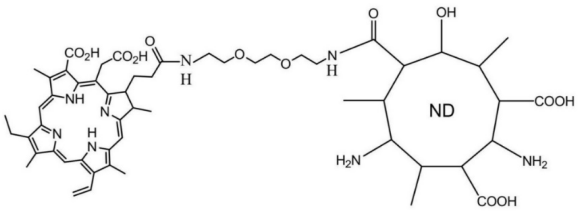

Figure 3: The structure of the $(Che6\text{-}spacer)_n$-ND conjugate.

Synthesis of $(FA\text{-}spacer)_n$ -ND-$(spacer\text{-}Che6)_n$ conjugate (Figure 4)

In the initial stage of FA-spacer-ND-spacer-Che6 conjugate synthesis the activation of carbonyl groups on FA and Che6 was conducted to promote the conjugation of activated carboxyl groups with free ND-EDA amino groups. The following reactions were conducted in nitrogen atmosphere in two separate 50 ml flasks: to FA (11.0 mg; 0.025 mmol) in the mixture of anhydrous DMSO (10 ml) and pyridine (1.5 ml) 1,1´-carbonyldiimidazole (4,37 mg; 0.027 mol) was added; to Che6 (14.9 mg; 0.025 mol) in the mixture of anhydrous DMSO (10 ml) and pyridine (1.5 ml) 1,1´-carbonyldiimidazole (4.37 mg; 0.027 mol) was added; further both mixtures were stirred for 1 hour at 25˚C on a magnetic stirrer. The ND-(EDA)n (50 mg) sediment was suspended in anhydrous DMSO (20 ml) in 50-ml round-bottomed flask in nitrogen atmosphere for 1 hour. Further, FA and DMAP (3 mg) were added into the reaction flask and stirred on a magnetic stirrer for 5 hours at room temperature, then Che6 was added and the mixture was stirred for 10 hours. After the termination of the reaction the resulting suspension was centrifuged (30 min at 10000 rev/min), and repeatedly washed with 5 ml of DMSO and 10 ml of ethyl ether in turns and centrifuged. The sediment of FA-spacer-ND-spacer-Che6 conjugate was used for spectral measurements. The scheme of synthesis of the FA-spacer-NA-spacer-Che6 conjugate with diamond nanoparticles is presented in (Figure 4).

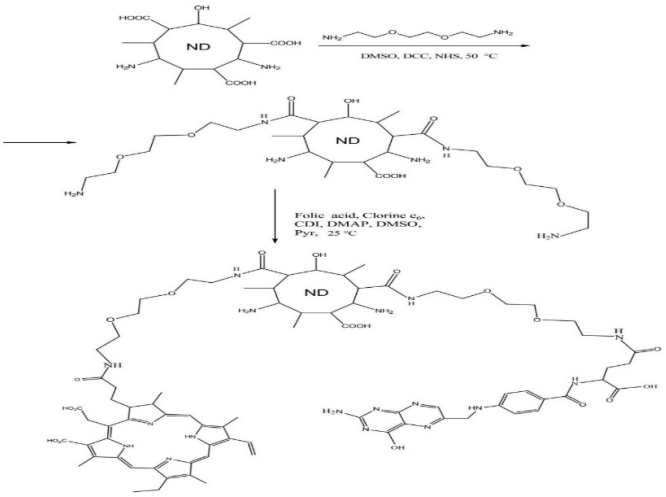

Figure 4: The scheme of $(FA\text{-}spacer)_n$-ND-$(spacer\text{-}Che6)_n$ conjugate synthesis.

Results and Discution

Spectral-Luminescent Characteristics of Che6-ND-FA Nanocomplex

To prove the presence of Che6 and FA in the nanoplatform composition and to study their influence on the properties of initial components, the investigation of spectral characteristics of the synthesized nanocomplex was conducted. (Figure 5) shows the spectra of optical density of suspensions of Che6-ND conjugate and Che6-ND-FA nanocomplex. As can be seen from the figure the typical Che6 absorption bands are observed, namely, the Soret

band around 400 nm and commonly used for photodynamic therapy absorption band within 640-680 nm which proves the conjugation of Che6 to nanoparticles. The observed absorption maximum in the nanocomplex suspension around 360 nm is determined by folic acid presence in the conjugate. It should be noted that in the experiments relatively low concentrations of ND (0.014 mass %) and, correspondingly, Che6 (4×10^{-7} mol/l) and FA (1×10^{-6} mol/l) were used. Strong light scattering by ND, however, interferes with absorption spectra measurements of conjugated Che6 and FA.

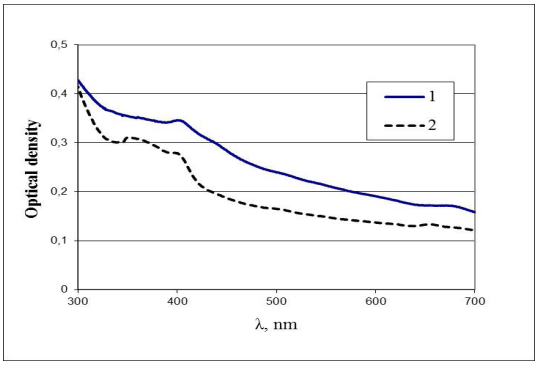

Figure 5: Optical density spectra of suspensions: Che6-ND conjugate (1) and Che6-ND-FA nanocomplex (2) in PBS with 5 % DMSO. The concentration of Che6 in samples is 4.0×10^{-7} mol/l, FA is 1.0×10^{-6} mol/l, the concentration of nanoplatform is 0.014 mass %.

To determine the influence of Che6 integration into ND-FA conjugate on electronic structure of Che6 photosensitizer the fluorescence spectra of Che6-ND-FA nanocomplex were investigated. (Figure 6) shows the fluorescence spectra of the nanocomplex in PBS with 5 % DMSO. As can be seen from the data presented, the fluorescence spectrum of Che6 bound to the nanocomplex differs inessentially from the spectrum of free Che6. After the conjugation the half-width of fluorescence spectrum of photosensitizer slightly decreases, its maximum shifts to the long-wavelength side and there is also some decrease of fluorescence intensity within the region of shoulder at 700 nm. The spectral investigations testify that conjugation of Che6 with ND-FA does not influence essentially its electronic structure.

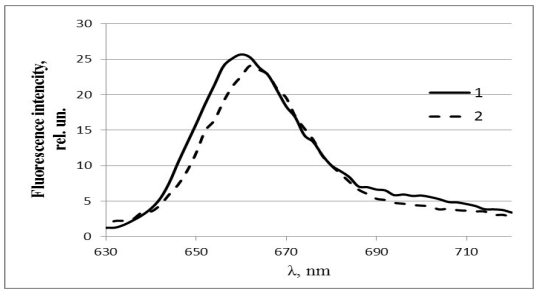

Figure 6: Fluorescence spectra of free (1) and nanocomplex-bound (2) Che6 in PBS with 5 % DMSO. The excitation wavelength is 405 nm. Che6 concentration in the sample is 4.0×10^{-7} mol/l, the concentration of the nanocomplex is 0.014 mass %.

Since the main purpose of our work is the development of a nanocomplex for photodynamic therapy, the investigation of the photosensitizing activity of Che6 in the composition of synthesized Che6-NG-FA nanoconjugate and its photostability in a biological medium is of great importance. The solution of human serum albumin (HSA) in PBS was used as such medium. (Figure 7) shows the data on photosensitizing action of free and conjugated Che6 resulting in tryptophan damage in HSA solution. The observed decrease of tryptophan fluorescence in samples under illumination proves photosensitized destruction of the indole ring of tryptophan in HSA solution by both free and conjugated Che6. As follows from the presented data, at the used concentrations of protein and nanoconjugate, Che6 is capable of photosensitizing the desctruction of HSA tryptophan under illumination, i.e. possesses photodynamic activity. It should be noted that at equal concentrations conjugated Che6 reveals essentially higher activity than free one.

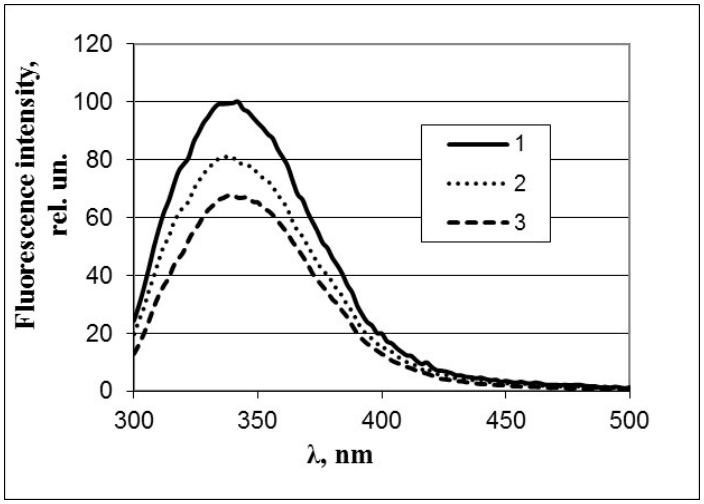

Figure 7: Spectra of HSA tryptophan fluorescence in the solution of free Che6 (1, 2) and in the suspension of Che6-ND-FA nanocomplex (1, 3) before (1) and after illumination of Che6 in a blue spectral region for 1.5 minutes (2, 3). The concentration of HSA in the solution and suspension is equal to 3.2×10^{-7} mol/l that corresponds to the concentration of conjugated Che6 in the suspension. The intensities of the fluorescence of coinciding initial spectra are normalized to 100 units in maximum. The excitation wavelength is 405 nm.

Photostability is a matter of major concern when developing photosensitizers for photodynamic therapy. In this connection the comparative investigation was conducted of photodestruction of free and conjugated Che6. The obtained data are presented in (Figure 8). The figure shows that at the illumination conditions applied the conjugated Che6 reveals higher photostability. Thus, the obtained results confirm that conjugated Che6 along with the increased photosensitizing activity reveals higher photostability compared to free Che6.

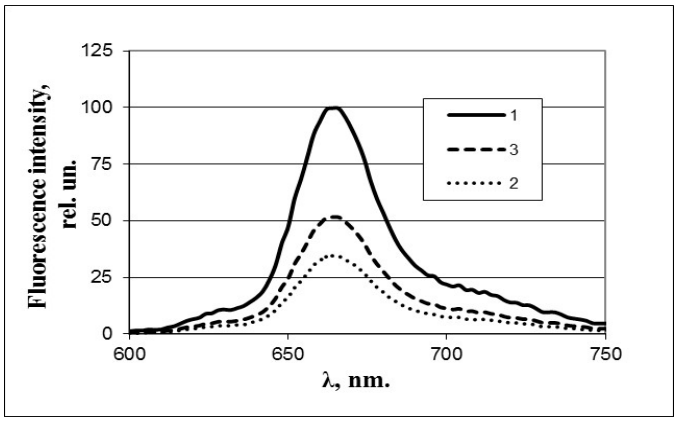

Figure 8: Che6 fluorescence spectra in the solution containing HSA and free Che6 (1, 3) and in the suspension containing HSA and ND-Che6-FA nanocomplex (1, 2) before (1) and after illumination of the Che6 by blue spectral region for 1.5 minutes (2, 3). HSA concentration in the solution and suspension is equal to 3.2×10^{-7} mol/l that corresponds to the concentration of conjugated Che6 in the suspension. The intensities of coinciding initial fluorescence spectra are normalized to 100 units in maximum. The excitation wavelength is 405 nm.

Che6-ND-FA Nanoconjugate Binding with Cells and Resulting Photosensitized Damage

The investigation of binding of the Che6-ND-FA conjugate with cells was conducted using the methods of transmitted light microscopy and laser scanning confocal microscopy. (Figure 9) shows the fluorescence microscopy images of HeLa cells before and after incubation with the nanoconjugate. As it can be seen, after incubation with Che6-ND-FA, the intensity of intracellular Che6 fluorescence significantly increases owing to the absorption of the nanoconjugate by the cells. The investigation of temporal dependence of mean intracellular fluorescence signal showed that this process was completed within 15-20 minutes. The data obtained using confocal microscopy under the excitation by argon laser line at 488 nm (Figure 10) also testifies the accumulation of the nanoplatform in cells. Cells at such illumination possess weak fluorescence originating from endogenous chromophores. Nanoplatform addition to the celullar medium results in the significant increase of intracellular fluorescence and after a certain length of time, certain decrease of fluorescence of intercellular medium is observed, presumably, due to the binding of the conjugate by the cells.

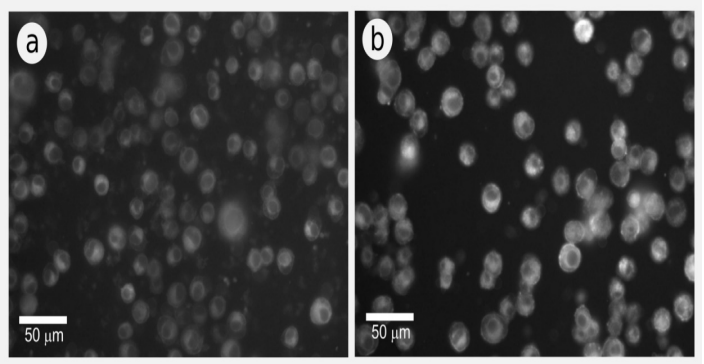

Figure 9: Fluorescence microscopy images of HeLa cells obtained immediately after (a) and in 20 minutes (b) after addition of Che6-ND-FA to the medium. Che6 concentration is 2.0×10^{-7} mol/l, nanoplatform concentration is 0.014 mass %.

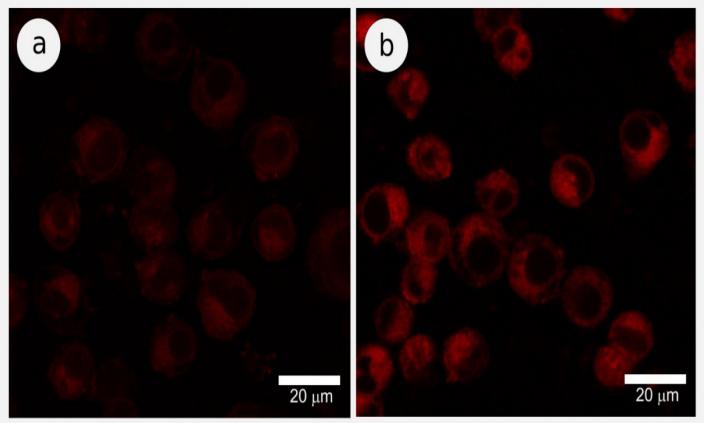

Figure 10: Laser scanning microscopy images of HeLa cells suspension: (a) - obtained immediately after introduction of ND-Che6-FA nanoplatform and (b) - after incubation with the nanoplatform in darkness for 20 minutes. The excitation wavelength is 488 nm. Che6 concentration is 2.0×10^{-7} mol/l, nanoplatform concentration is 0.014 mass %.

(Figure 11) shows fluorescence spectra of separate cells obtained by microspectroscopy technique using laser scanning confocal microscope. The spectra are similar to that of Che6. As can be seen from (Figure 11), in conjugate treated cells Che6 fluorescence was registered having its maximum at 663 nm and a shoulder around 700 nm.

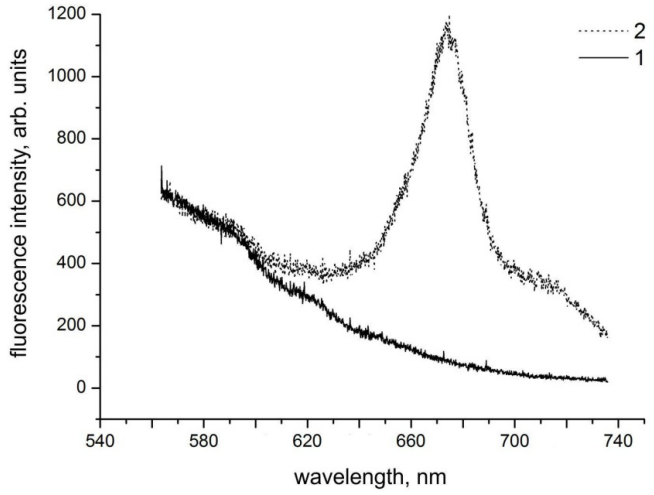

Figure 11: Fluoresence spectra of HeLa cell interior in buffered physiological solution containing Che6-ND-FA conjugate recorded by microspectroscopy technique immediately after the introduction of the conjugate into the medium (1) and in 30 minutes (2). The excitation wavelength is 488 nm.

The data obtained confirm that Che6-ND-FA conjugate interacts with HeLa cells. The mechanism of this interaction is of scientific and practical interest for PDT treatment using the synthesized conjugate. The above-given data testifies that folic acid provides binding of the conjugate with cells and its subsequent delivery into the cells. The mentioned factors allow one to suppose the possibility of photosensitized damage of cells bound with the conjugate as a result of their illumination. To check up this assumption the death of cells photosensitized by the conjugate was investigated. Malignant transformed HeLa cells expressing folate receptors were used. The cells were cultivated in 199 medium and were used at the logarithmic stage of their growth. For analysis of photosensitized death of cells, 0.02 ml of suspension of Che6-ND-FA nanoplatform (0.14 mass % of nanoplatform containing 2.0×10^{-6} mol/l of Che6) was added to 0.2 ml of cell suspension (2.0×10^{5} cells/ml). The samples were incubated for 30 minutes allowing binding the nanoplatform to the cells. The illumination of samples was performed in HUNK camera at the thickness of optical layer of 1 mm by the light of KGM lamp (150 W) through the water filter and optical bandpass filter FS4 transmitting radiation within 370-430 nm region. The incident power density of the radiation on the sample within the chlorine absorption region of Soret band was 10 mW/cm^2.

The death of cells (necrotic) was determined by means of Propidium Iodide (PI), which was performed as follows. Illuminated cells were incubated for 60 minutes in darkness and then PI solution of 2.0×10^{-5} mol/l was added into incubation medium. In following 30 minutes fluorescence microscopy images of cells were registered using corresponding filter set transmiting PI fluorescence. (Figure 12) shows the images of HeLa cells illuminated in a suspension containing Che6-ND-FA conjugate and PI. As can be seen, the sample reveals photosensitizing influence of the conjugate since numerous dead cells appear. This dying proves the damage of cellular membranes that allows PI to enter into the cells and bind with nucleic acid with the formation of a fluorescent complex. The percentage of dead cells depends on the intensity of photodynamic action. In (Table 2) the data are given on the dependence of dead cells percentage on the duration of sample illumination. As follows from the data, conjugated Che6 effectively induces photosensitized necrosis of tumor HeLa cells in *in vitro* at relatively low concentration (2.0×10^{-7} mol/l).

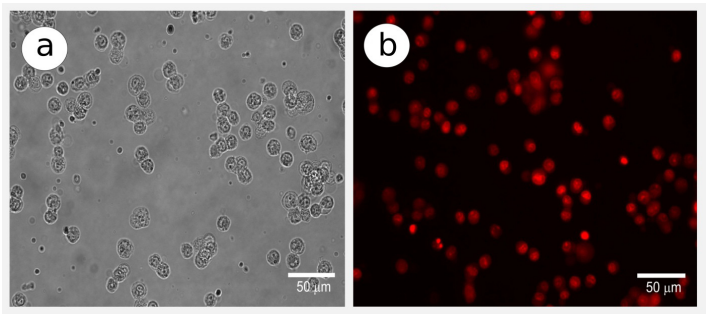

Figure 12: Microphotos of HeLa cells obtained in transmitted (a) and PI fluorescence (b) light revealing photosensitizing effect of the conjugate. The duration of sample illumination is 3 minutes.

Illumination time, min.	0	2	4	6	8	10
% of dead cells	8,2	15,1	28,6	45,3	69,1	91,3

Table 2: The dependence of Che6-ND-FA nanoconjugate bound HeLa cells death percentage on cell illumination duration.

Conclusions

On the basis of the obtained experimental results as well as numerous literature data, we have developed the scheme for synthesis of photodymanically active selective Che6-ND-FA complex and have performed the synthesis. The experimental investigations have shown that Che6 being a part of Che6-diamond nanoparticles - folic acid nanocomplex possesses photodynamic activity, and folic acid provides means of binding of the nanocomplex to folate receptor expressing cells (Figure 13).

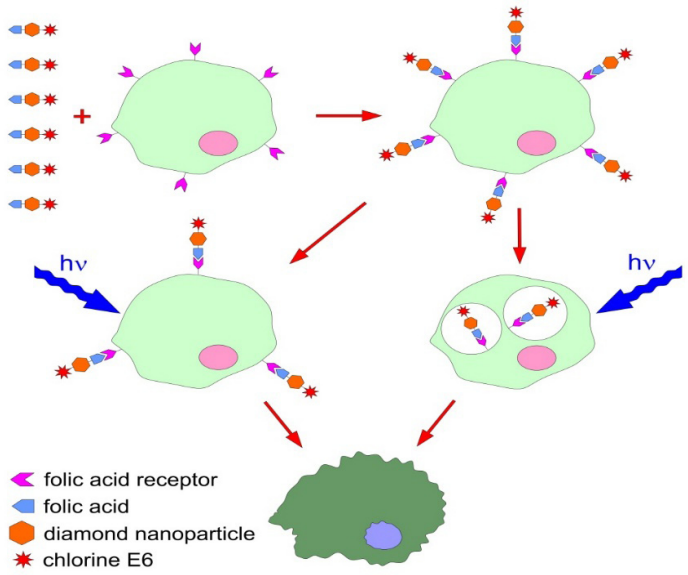

Figure 13: Folate-mediated delivery of a therapeutic agent into folate receptor positive tumor cells and their photosensitized death.

At present multiple data testify that the receptor-mediated transportation of folates occurs on the basis of endocytosis [25-28]. Both the mechanism of the receptor-mediated endocytosis of folates into cells and the mechanism of folate receptor work are still the subject of active investigations and discussions. It is generally accepted that the receptor works through recirculation mechanism including multiple passage from plasmatic membrane into endosomes and backwards, binding and releasing ligand molecules. The efficiency of such work is determined by many factors: quantity of receptors on the cell surface, extracellular concentration of folate ligands, affinity of folates to the receptors, velocity of energy-dependent endocytosis, velocity of the release of receptor molecules from endosomes, the ability of receptor repeated integration into cellular membrane and so on. It is possible to suppose that a part of folate receptor associated conjugates of folic acid with photosensitizer enters the cell by receptor-mediated endocytosis (right side of Figure 13), while the other part remains on the cell surface (left side of the Figure 13). Based on this assumption, two types of therapeutic strategy can be proposed. Molecules of photosensitizer, which require the access to intercellular targets, can be delivered into cytosol in large amounts by means of endocytosis, while the molecules of photosensitizer, which can or must fulfill their functions outside the cell, will accumulate on the surface of tumor cell due to stationary population of folate receptors (Figure 13). At illumination of cells with the bound nanoconjugate their selective death will occur without any influence on healthy cells. The behavior of the proposed folate receptor selective photodynamically active conjugate requires further investigation and development. Taking into account the results obtained in the present study there is no doubt that this approach is perspective for clinical medicine.

References

1. Reddy JA, Low PS (1998) Folate-mediated targeting of therapeutic and imaging agents to cancers. Critical reviews in therapeutic drug carrier systems 15: 587-627.
2. Leamon CP, Jackman AL (2008) Exploitation of the folate receptor in the management of cancer and inflammatory disease. Vitamins and Hormones 79: 203-233.
3. Kamen BA, Smith AK (2004) A review of folate receptor alpha cycling and 5-methyltetragidrofolate accumulation with an emphasis on cell models *in vitro*. Advanced Drug Delivery Reviews 56: 1085-1097.
4. Rettig W, Garin-Chesa P, Beresford H, Oettgen HF, Melamed MR, et al. (1988) Cell-surface glycoproteins of human sarcomas: differential expression in normal and malignant tissues and cultured cells. Proceedings of the National Academy of Sciences of the United States of America 85: 3110-3114.
5. Weitman SD, Lark RH, Coney LR, Fort DW, Frasca V, et al. (1992) Distribution of the folate receptor (GP38) in normal and malignant cell lines and tissues. Cancer Research 52: 3396-3401.
6. Leamon CP, Low PS (1993) Membrane folate-binding proteins are responsible for folate-protein conjugate endocytosis into cultured cell. Biochemical Journal 291: 855-860.
7. Lu Y, Low PS (2002) Folate-mediated delivery of macromolecular anticancer therapeutic agents. Advanced Drug Delivery Reviews 54: 675-693.
8. Wang S, Low PS (1998) Folate-mediated targeting of antineoplastic drugs, imaging agents, and nucleic acids to cancer cells. Journal of Controlled Release 53: 39-48.
9. Van Dongen GAMS, Vrouenraets MB, Visser GWM (2001) Targeting of photosensitizers to head and neck tumours by the use of monoclonal antibodies. Clinical Otolaryngology & Allied Sciences 26: 339.
10. Schneider R, Schmitt F, Frochot C, Fort Y, Lourette N, et al. (2005) Design, synthesis, and biological evaluation of folic acid targeted tetraphenylporphyrin as novel photosensitizers for selective photodynamic therapy. Bioorganic & Medicinal Chemistry 13: 2799-2808.
11. Bareford LM, Swaan PW (2007) Endocytic mechanisms for targeting drug delivery. Advanced Drug Delivery Reviews 59: 748-758.
12. Lu Y, Low PS (2002) Folate-mediated delivery of macromolecular anticancer therapeutic agents. Advanced Drug Delivery Reviews 54: 675-693.
13. Hilgenbrink AR, Low PS (2005) Folate receptor-mediated drug targeting: from therapeutics to diagnostics. Journal of Pharmaceutical Sciences 94: 2135-2146.
14. Lee RJ, Low PS (1995) Folate-mediated tumor cell targeting of liposome-entrapped doxorubicin *in vitro*. Biochimica et Biophysica Acta 1233: 134-144.
15. Li WT (2013) Nanoparticles for Photodynamic Therapy. Handbook of Biophotonics. Vo2: Photonics for Health Care Published by Wiley-VCH Verglag GmbH&Co.KGaA : 321-336.
16. Lapina VA, Bushuk SB, Pavich TA, Vorobey AV (2016) New generation of photosensitizers: conjugates of chlorine e6 with diamond nanoparticles. Journal of Applied Spectroscopy 83: 344-349.

17. Lapina VA, Vorobey AV, Pavich TA, Opitz J (2013) Targeting diamond nanoparticles into folate-receptor expressing HeLa cells. Journal of Applied Spectroscopy 80: 414-418.

18. Mkandawire M, Pohl A, Gubarevich T, Lapina V, Appelhans D, et al. (2009) Selective targeting of green fluorescent nanodiamond conjugates to mitochondria in HeLa cells. Journal of Biophotonics 2: 596-606.

19. Opitz J, Mkandawire M, Sorge M, Rose N, Rudolph M, et al. (2010) Green fluorescent nanodiamond conjugates and their possible applications for biosensing. Proceedings of SPIE 7759: 775914.

20. Gubarevich TM, Gorbacheva AN, Karoza AG, Lapina VA (2008) IR-spectroscopy of the Surface State of Detonation Nanodiamonds. Proceedings of the 3rd Internatoinal Symposium. Detonation nanodiamonds: technology, properties and applications. St. Petersburg, Russia: 99-102.

21. Huang X, Tian XJ, Yang WL, Ehrenberg B, Chen JY (2013) The conjugates of gold nanorods and chlorin e6 for enhancing the fluorescence detection and photodynamic therapy of cancers. Physical Chemistry Chemical Physics 15: 15727-15733.

22. Gravier J, Schneider R, Frochot C, Bastogne T, Schmitt F, et al. (2008) Improvement of meta-tetra(Hydroxyphenyl)chlorine-Like Photosensitizer Selectivity with Folate-Based Targeted Delivery. Synthesis and *in vivo* Delivery Studies. Journal of Medicinal Chemistry 51: 3867-3877.

23. Kulakova II (2004) Surface chemistry of nanodiamonds. Physics of the Solid State 46: 636-643.

24. Wang S, Luo J, Lantrip DA, Waters DJ, Mathias CJ (1997) Design and Synthesis of [111In] DTPA-Folate for Use as a Tumor-Targeted Radiopharmaceutical. Bioconjugate Chemistry 8: 673-679.

25. Kamen BA, Smith AK (2000) A review of folate receptor alpha cycling and 5-methyltetragidrofolate accumulation with an emphasis on cell models *in vitro*. Advanced Drug Delivery Reviews 56: 1085-1097.

26. Leamon CP, Low PS (1991) Delivery of macromolecules into living cells: A method that exploits folate receptor endocytosis. Proceedings of the National Academy of Sciences of the United States of America 88: 5572-5576.

27. Lee RJ, Low PS (1994) Delivery of liposomes into cultured KB cell via folate receptor-mediated endocytosis. Journal of Biological Chemistry 269: 3198-3204.

28. Antony AC (1996) Folat receptors. Annual Review of Nutrition 16: 501-521.